Journal of Medicinal Chemistry

Article

Far-red Light-activatable Prodrug of Paclitaxel for the Combined Effects of Photodynamic Therapy and Site-specific Paclitaxel Chemotherapy

Pritam Thapa, Mengjie Li, Moses Bio, Pallavi Rajaputra, Gregory Nkepang, Yajing Sun, Sukyung Woo, and Youngjae You

J. Med. Chem., **Just Accepted Manuscript** • DOI: 10.1021/acs.jmedchem.5b01971 • Publication Date (Web): 14 Mar 2016

ACS Publications

Journal of Medicinal Chemistry is published by the American Chemical Society. 1155 Sixteenth Street N.W., Washington, DC 20036

Far-red Light-activatable Prodrug of Paclitaxel for the Combined Effects of Photodynamic Therapy and Site-specific Paclitaxel Chemotherapy

Pritam Thapa, Mengjie Li, Moses Bio, Pallavi Rajaputra, Gregory Nkepang, Yajing Sun, Sukyung Woo, Youngjae You*

College of Pharmacy, University of Oklahoma Health Sciences Center, Oklahoma City, OK, 73117

Key words: Combination Therapy, Aminoacrylate, Light-activatable Prodrug, Singlet Oxygen, Photodynamic Therapy, Chemotherapy, Paclitaxel

ABSTRACT

Paclitaxel (PTX) is one of the most useful chemotherapeutic agents approved for several cancers, including ovarian, breast, pancreatic, and non-small cell lung cancer. However, it causes systemic side effects when administered parenterally. Photodynamic therapy (PDT) is a new strategy for treating local cancers using light and photosensitizer. Unfortunately, PDT is often followed by recurrence, due to incomplete ablation of tumors. To overcome these problems, we prepared the far-red light-activatable prodrug of PTX by conjugating photosensitizer *via* singlet oxygen-cleavable aminoacrylate linker. Tubulin polymerization enhancement and cytotoxicity of prodrugs were dramatically reduced. However, once illuminated with far-red light, the prodrug effectively killed SKOV-3 ovarian cancer cells through the combined effects of PDT and locally released PTX. Ours is the first PTX prodrug that can be activated by singlet oxygen using tissue penetrable and clinically useful far-red light, which kills the cancer cells through the combined effects of PDT and site-specific PTX chemotherapy.

INTRODUCTION

Paclitaxel (PTX), first isolated from *Taxus brevifolia* bark, is one of the most important chemotherapeutic agents.[1, 2] This drug promotes tubulin polymerization and stabilizes the microtubules, preventing depolymerization.[3] PTX is used as the first-line therapy for various cancers, including ovarian cancer,[4-6] breast cancer,[7, 8] and non-small-cell lung cancer,[9, 10] and is used for both adjuvant and neoadjuvant chemotherapy.[11-15] Numerous prodrug forms of PTX have been developed and studied. These prodrugs include enzyme cleavable/self-immolative prodrugs, antibody-directed enzyme prodrugs, albumin conjugates, and PAMAM dendrimer conjugates, to reduce systemic side effects from chemotherapy.[16-22] However, dose-limiting systemic side effects are still considered a major problem accompanying the systemic exposure of PTX.

Photodynamic therapy (PDT) is based on the use of visible or near IR light and a photosensitizer. PDT was approved for the treatment of several cancers, including bladder, lung, and esophageal cancers.[23-27] PDT works when light of an appropriate wavelength activates the photosensitizer to produce reactive oxygen species, mainly singlet oxygen.[28] Singlet oxygen is a toxic species that can kill cells by apoptosis and/or necrosis.[29] However, disease recurrence stemming from the cells surviving after PDT treatment is a significant problem,[30, 31] which partly is due to the short half-life (~ 10-320 ns) and limited diffusion distance (~10-55 nm) of singlet oxygen in cells.[32, 33] Most recently, singlet oxygen has been applied to prodrug activation.[34-39]

We proposed the novel combined therapy of photodynamic and site-specific chemotherapy using unique conjugates of photosensitizers and anticancer drugs to ablate localized tumors without causing systemic side effects.[40-43] The two functional moieties

are connected with a singlet oxygen cleavable linker. Upon activation of the photosensitizer with deep tissue-penetrable visible and far-red light, the conjugate generates singlet oxygen that triggers immediate PDT damage and then cleaves the linker, releasing the chemotherapeutic drugs only at the site of illumination. Our study of various singlet oxygen-cleavable linkers led to the discovery of an efficient aminoacrylate linker.[44, 45] Utilizing this aminoacrylate linker, our group prepared conjugates of model drugs, including combretastatin-A4 (CA4)[41-43] and SN-38.[40] Both of these compounds have a phenolic group and effectively released parent drugs with visible or far-red light illumination.

The goals of the present study were 1) to prepare a far-red light activatable prodrug of PTX by conjugating PTX with Pc (silicon phthalocyanine, a fluorescence photosensitizer) *via* our aminoacrylate linker, 2) to demonstrate its PTX release profiles, and 3) to evaluate its *in vitro* activity using SKOV-3 ovarian cancer cells. There are some reports of photoactivatable prodrugs in which UV and visible, near-IR light were used to release PTX from various delivery forms.[46-50] However, our study is, to our knowledge, the first to report the use of far-red light to release PTX from a prodrug *via* singlet oxygen generation. This approach permits the combined treatment of PDT and site-specific PTX chemotherapy for more complete ablation of cancer cells.

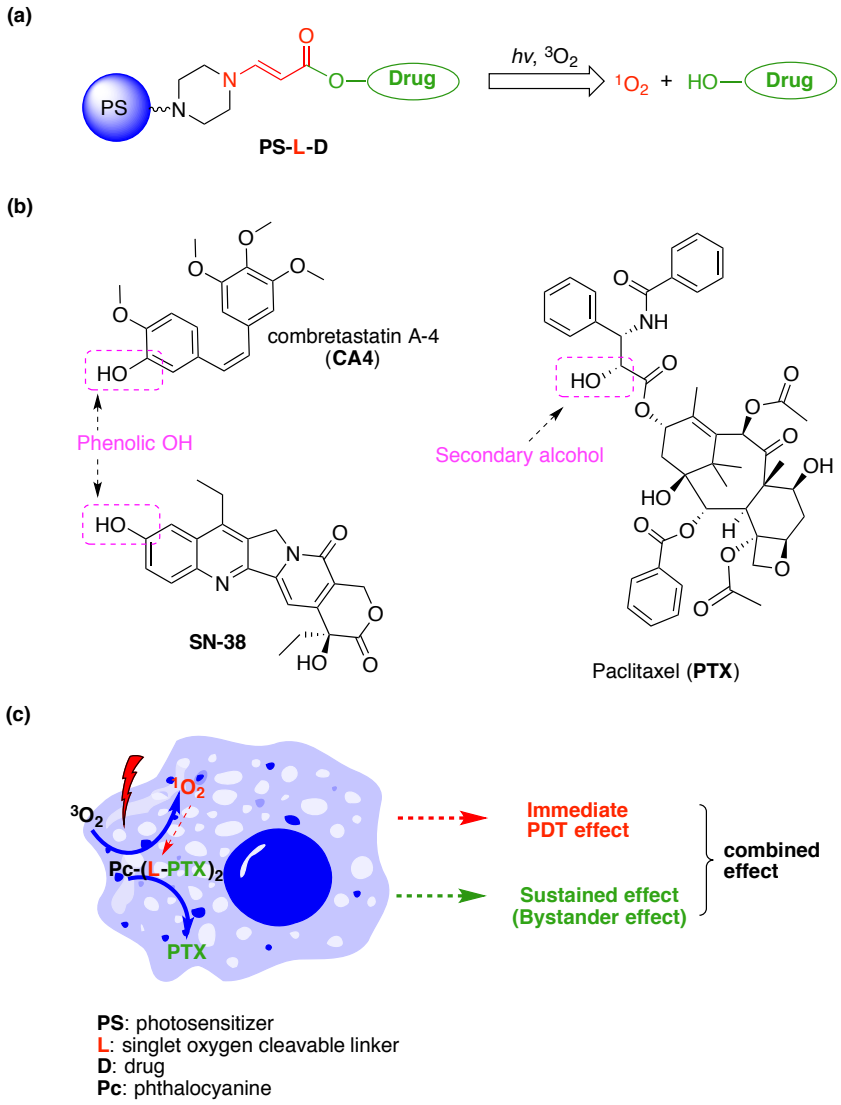

Figure 1. (a) Light-activatable prodrug *via* singlet oxygen-cleavable aminoacrylate linker, (b) Structures of anticancer drugs, CA4, SN-38, and PTX, (c) Schematic presentation of singlet oxygen-cleavable prodrugs of PTX expressing the combined effects of PDT and site-specific PTX chemotherapy.

RESULTS AND DISCUSSION

Design and synthesis of cleavable and non-cleavable PTX prodrugs, 4 (Pc-(L-PTX)$_2$) and 5 (Pc-(NCL-PTX)$_2$). We designed two PTX prodrugs with a fluorescence

photosensitizer, silicon phthalocyanine (Pc; Scheme 1). Compound **4** is the singlet oxygen-cleavable PTX prodrug. Thus, it was expected to produce combined effects of PDT and site-specific chemotherapy (Fig. 1c). However, compound **5** is a pseudo-prodrug of **4** that does not release PTX, even after illumination. Thus, compound **5** was expected to produce only PDT effects after illumination. For the conjugation of PTX with Pc, the most reactive hydroxyl group, 2'-OH, was selected due to its critical role for the binding of PTX to tubulin. There have been several reports of the importance of 2'-OH for the cytotoxic effects of PTX; 2'-OH also plays a critical role in stabilizing tubulin polymerization by binding with the D26 region within the microtubule binding site.[51-54] By modifying 2'-OH, we could attenuate the activity of PTX. This activity attenuation is an essential characteristic for estabilishing prodrug character.

The two PTX prodrugs were successfully synthesized through a facile and short scheme (Scheme 1), following our previous methods with a minor modification.[42, 45] For the synthesis of **4**, first PTX intermediate **1**[55] was prepared by the Steglich esterification, in which PTX was reacted with propiolic acid in the presence of DCC and DMAP to obtain **1** in 86% yield. Compound **1** was then reacted with Pc intermediate **2**[42] in THF to produce compound **4** as a blue solid in 46% yield. Similarly, **5** was obtained by the preparation of PTX intermediate **3**, according to the previously reported method,[56, 57] and conjugating it with Pc intermediate **2**. In brief, PTX was reacted with succinic anhydride in the presence of pyridine to obtain compound **3**. Using an amide coupling reaction, compound **3** was conjugated with Pc intermediate **2** to give compound **5** as a blue solid in 57% yield.

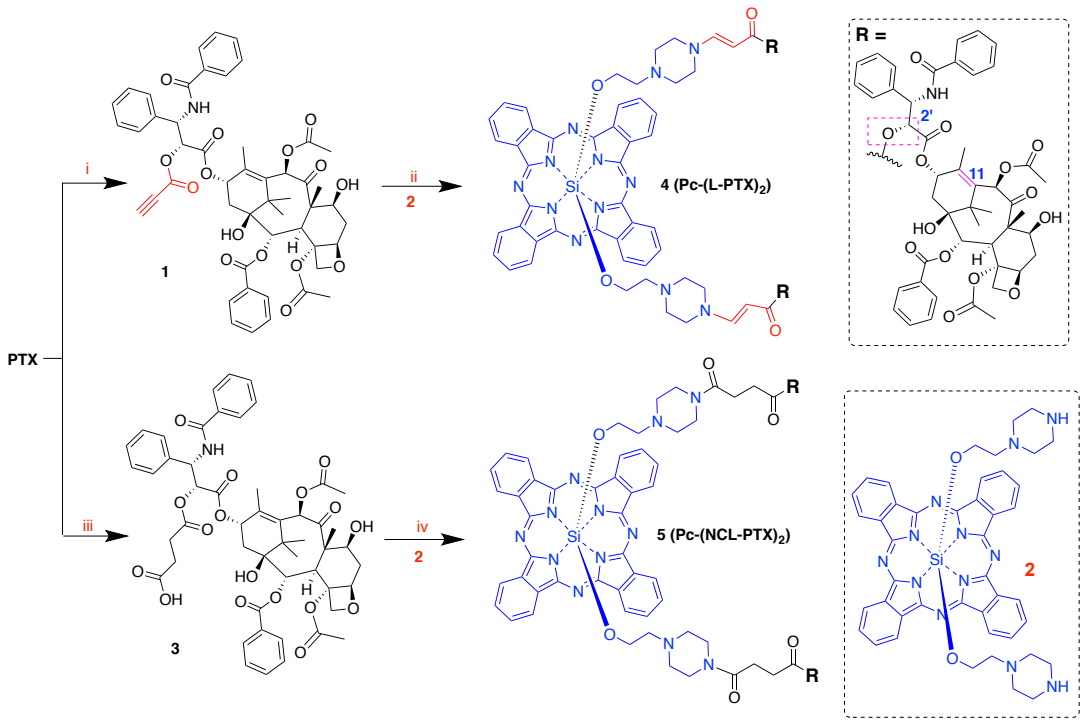

Scheme 1. Synthesis of compound **4** and **5**; Reagents and Conditions: i) Propiolic acid, DCC, DMAP, THF, 0 °C, 3 h, 86%; ii) **2**, THF, 0 °C, 1.5 h, 46%; iii) Succinic anhydride, Dichloromethane, r.t., 24 h, 93%; and iv) **2**, EDC·HCl, HOBt, Et_3N, Dichloromethane, 0 °C for 0.5 h→ r.t. for 3.5 h, 57%.

UV/Vis Absorption and Fluorescence Emission Spectra, and $LogD_{7.4}$. To evaluate the potential for UV-Vis detection and fluorescence imaging of these two prodrugs, the UV/Vis absorption and fluorescence emission of both prodrugs were determined in 5% DMSO in ACN (Fig. 2). UV/Vis absorption spectra (Fig. S13) showed a sharp Q-band at 672 nm for both prodrugs. This is a typical peak for the Pc chromophore. The graph plotted between the concentration and absorbance at the Q-band exhibited linearity following the Beer Lambert law in the tested concentrations, ranging from 0.5 to 8 μM. The molar absorption co-efficiency at 672 nm was 192,600 and

251,000 $M^{-1}cm^{-1}$ for **4** and **5**, respectively, which is high and thus can be useful for UV-Vis detection in the far-red region. These results indicate that the conjugation of Pc with two PTXs with these linkers had no negative effect on the absorption properties of the Pc chromophore. Similarly, the fluorescence spectra showed the λ_{flu} at 678 nm and 677 nm for **4** and **5**, respectively. This finding indicates that conjugation did not significantly shift the emission of Pc fluorophore in the prodrugs. The absorption peak at 285 nm of **4** is attributed to the aminoacrylate linker.[58] These two prodrugs have appropriate absorption and emission profiles for fluorescence imaging *in vitro* and *in vivo*. The prodrugs were also lipophilic. Partition coefficients, as denoted by $logD_{7.4}$, were > 3.1 for both compounds **4** and **5**.

(a)

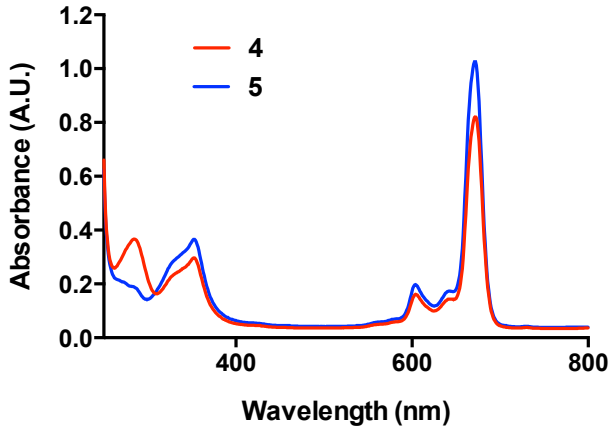

(b)

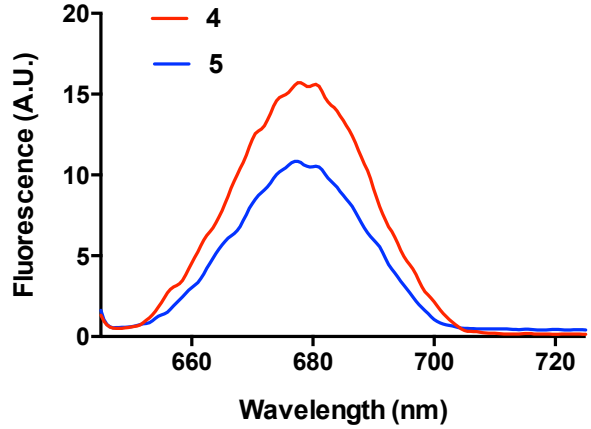

(c)

Compound	λ_{abs} (nm) [ε ($M^{-1}\cdot cm^{-1}$)]				λ_{em} (nm)	$logD_{7.4}$
4	285 (76,100)	353 (63,300)	604 (31,200)	672 (192,600)	678	> 3.1
5	-	352 (82,700)	604 (41,400)	672 (251,000)	677	> 3.1

Figure 2. UV/Vis (a) and fluorescence (b) spectra of **4** and **5** in 5% DMSO/ACN, (c) Spectral and $logD_{7.4}$ values of **4** and **5**.

Stability of Prodrugs 4 and 5 under Dark Conditions. Because there are two ester bonds in both prodrugs (Scheme 1), we wanted to evaluate their stability against hydrolysis in complete medium in the dark. The prodrugs in the medium were quantified at various time points (t = 2-168 h; Fig. 3) using HPLC. The results were compared with those of the initial sample (t = 0). Compound **4** was stable for 96 h with a less than 7% decrease (Fig. 3c). Similarly, **5** was stable for 24 h with only 4% loss. After 96 h, 14% of the prodrug compound was lost. The presence of the saturated ester bonds in **5** may account for its marginally lower stability (p = 0.21) than **4**, which has the conjugated ester bond. Overall, the hydrolysis of these two prodrugs in the media was not rapid without illumination.

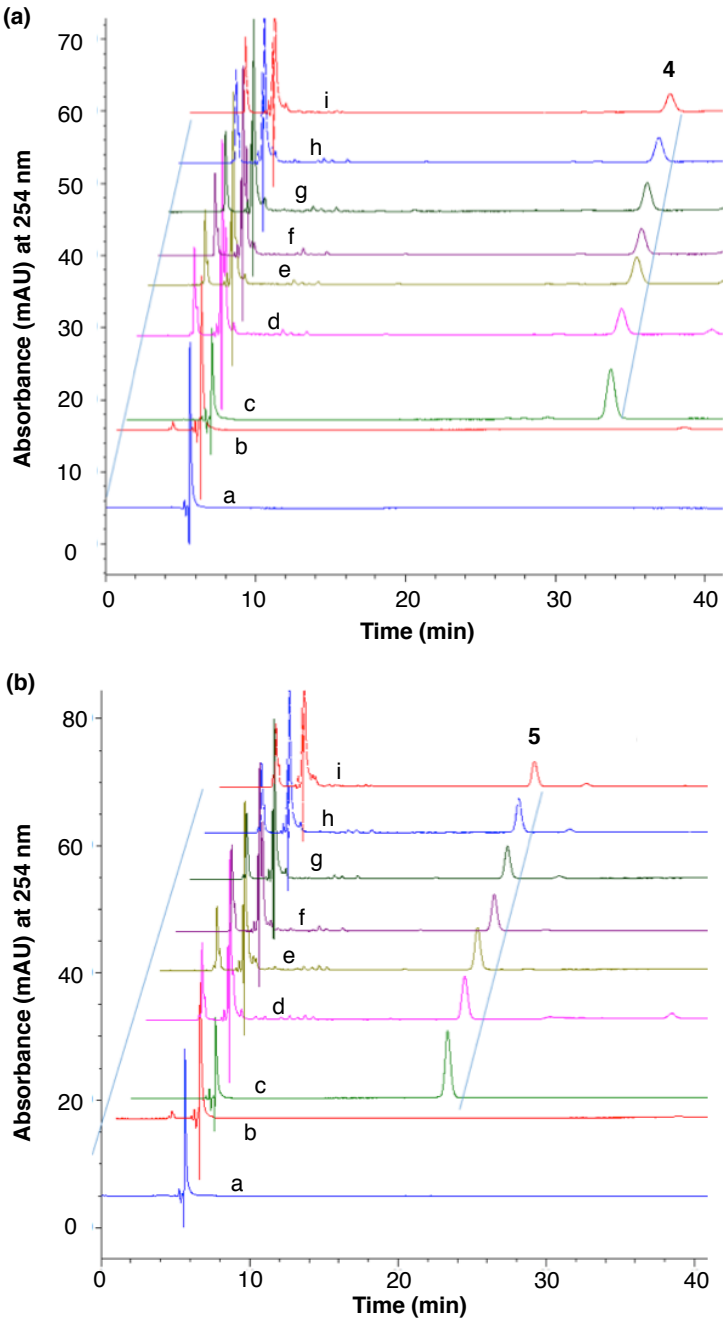
(a)
Absorbance (mAU) at 254 nm
Time (min)
4
i
h
g
f
e
d
c
b
a
(b)
Absorbance (mAU) at 254 nm
Time (min)
5
i
h
g
f
e
d
c
b
a

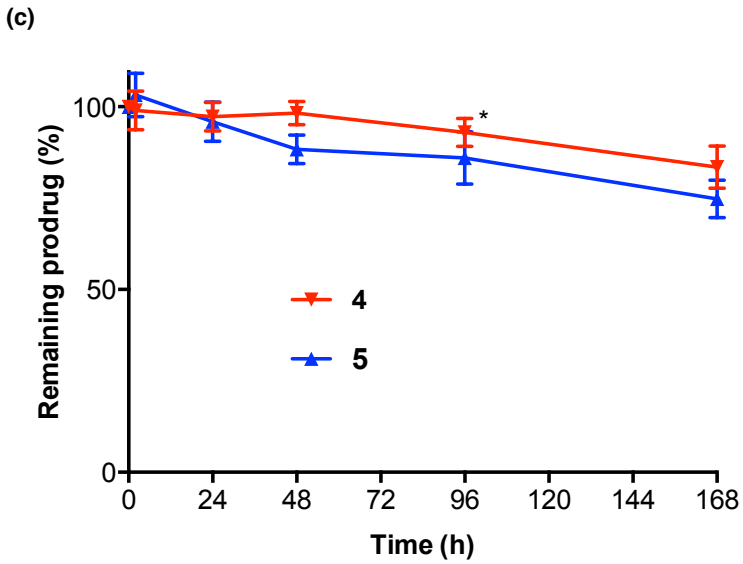

Figure 3. HPLC Chromatograms of **4** (a) and **5** (b); a: DMSO alone, b: extracted from the medium without any prodrug, c: prodrug in 5% DMSO in ACN (10 μM), d - i: the prodrug extract from the medium (10 μM) at 0, 2, 24, 48, 96, and 168 h, respectively, (c) Remaining prodrug (%) at various time points from three experiments (* $p < 0.05$).

Tubulin Polymerization Effect of 4 and 5. The two prodrugs were anticipated to be significantly less active than PTX. Since PTX promotes tubulin polymerization to make microtubules, we tested **4** and **5** with a tubulin polymerization assay kit. In this assay, fluorescence increases represent increased tubulin polymerization. We expected that the introduction of bulky groups (Pc-L and Pc-NCL) to 2'-OH of PTX (Scheme 1), which is important for tubulin binding, would reduce the tubulin polymerization activity of PTX. Indeed, both compounds did not show enhancement in tubulin polymerization, unlike PTX (Fig. 4a). With PTX, the tubulin polymerization was rapid and reached a maximum at ~16 min. Combretastatin A-4 (CA4), a tubulin polymerization

inhibitor,[59,60,61] almost completely prevented the polymerization for 1 h. However, the curves of **4** and **5** were similar to that of the control, reaching a plateau at ~ 40 min. Even at higher concentrations (10x), these prodrugs did not show any significant enhancement in tubulin polymerization (Fig. 4b). The activity of PTX for tubulin polymerization was successfully masked in both prodrugs. Next, we explored the tubulin polymerization effect of irradiated samples of compounds **4** and **5** (Fig. S15). As anticipated, we observed that the tubulin polymerization effect of irradiated sample **4** was significantly increased, while there was not much change for the irradiated sample **5**. This further supports our finding that there was a significant release of PTX from the prodrug **4** upon irradiation with far-red light.

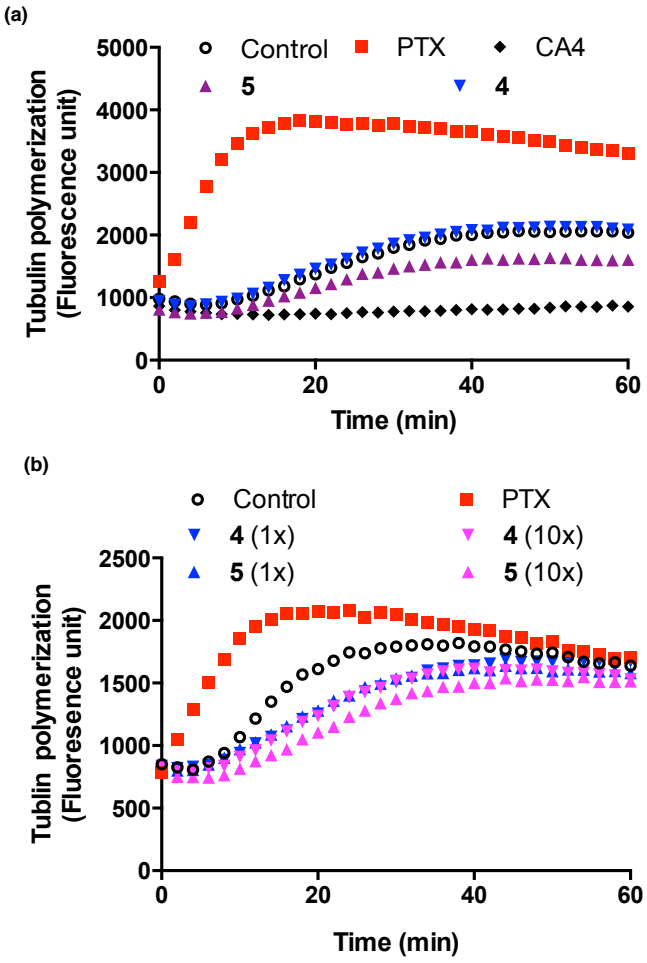

Figure 4. (a) Effects of **4** and **5** at 3 μM on tubulin polymerization, and (b) Effects on tubulin polymerization at higher concentrations of prodrugs (1x = 3 μM and 10x = 30 μM). Control = vehicle only.

Photocleavage of 4 and 5 in the Complete Medium. We first wanted to determine if the intact PTX could be released from prodrug **4** upon illumination, because the release of secondary alcohol from the aminoacrylate linker had not yet been confirmed and the double bond (at C11 and C12) of the PTX could be susceptible to oxidation by singlet oxygen. We also wanted to determine the rate of PTX release from the prodrugs. PTX was quantified after illumination of these prodrugs with 690 nm laser light at 5.6 mW/cm^2. The prodrug samples (10 μM) were prepared in DMEM with 5% FCS. The prodrug solution (0.5 mL) was placed in a clear glass beaker (3-cm diameter) to increase the area of the illumination. The entire beaker was illuminated with the laser from above for 10, 20, and 30 min. PTX was then extracted with dichloromethane, quantified by HPLC, and compared with the standard PTX solution.

We were able to detect intact PTX from the illuminated solution of compound **4**. A peak at the same retention time with standard PTX itself was observed from the illuminated prodrug solution at 11 min (Fig 5b). We further confirmed the peak with high-resolution mass spectroscopy after collecting the peak fraction from HPLC (Fig. S14). The release of PTX by the illumination was rapid. After the illumination for 10 and 30 min, about 83% and 93% of PTX was released from the prodrug (Fig. 5 inset). Extraction efficiency (EE) of PTX from the complete media was 74 ± 6%. However, we could not detect PTX from the illuminated sample of **5** due to the absence of the singlet oxygen-cleavable linker (Fig. 5f).

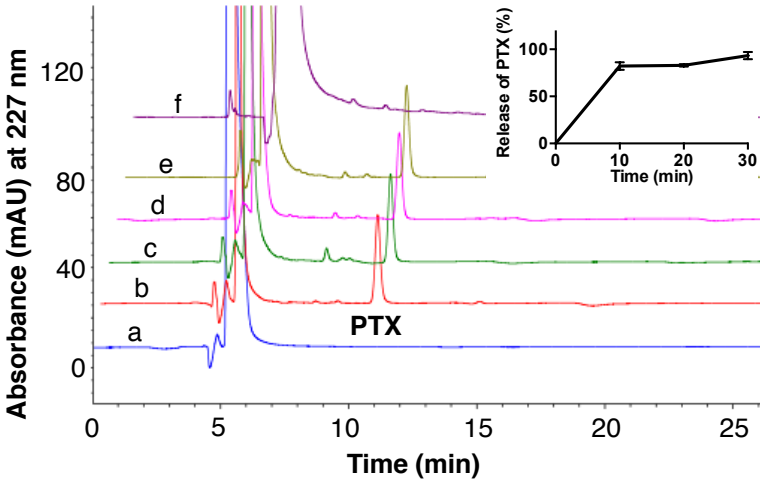

Figure 5. HPLC chromatograms of (a) 2.5% DMSO in ACN; (b) PTX (20 μM) in the media; (c-e) **4** (10 μM) in the media illuminated with 690 nm at 5.6 mW/cm^2 for 10, 20, and 30 min; (f) **5** (10 μM) in the media illuminated for 30 min; (Inset) PTX release (%) after illumination of **4**.

Subcellular Localization Compared with Tubulin Tracker Green. Tubulin polymerization assay showed that the prodrugs **4** and **5** did not promote tubulin polymerization. We assumed that these two prodrugs do not specifically bind to polymerized tubulin inside cells due to the steric bulkiness at 2'-OH. To confirm the tubulin polymerization assay results in cells, we performed a subcellular localization study with the confocal microscope. The prodrugs have an excellent fluorophore (Pc) that can be easily visualized through fluorescence imaging. To specifically stain polymerized tubulin (microtubules) inside cells, tubulin tracker green was used. SKOV-3 cells were incubated with either prodrug. Then, tubulin tracker green was added 45-60 min before images were captured. We first obtained three sequential images: bright-field (i) → tubulin tracker green fluorescence (ii) → prodrug fluorescence image (iii) (Fig. 6). Then, we overlapped the images of tubulin tracker green with **4** or **5** (iv).

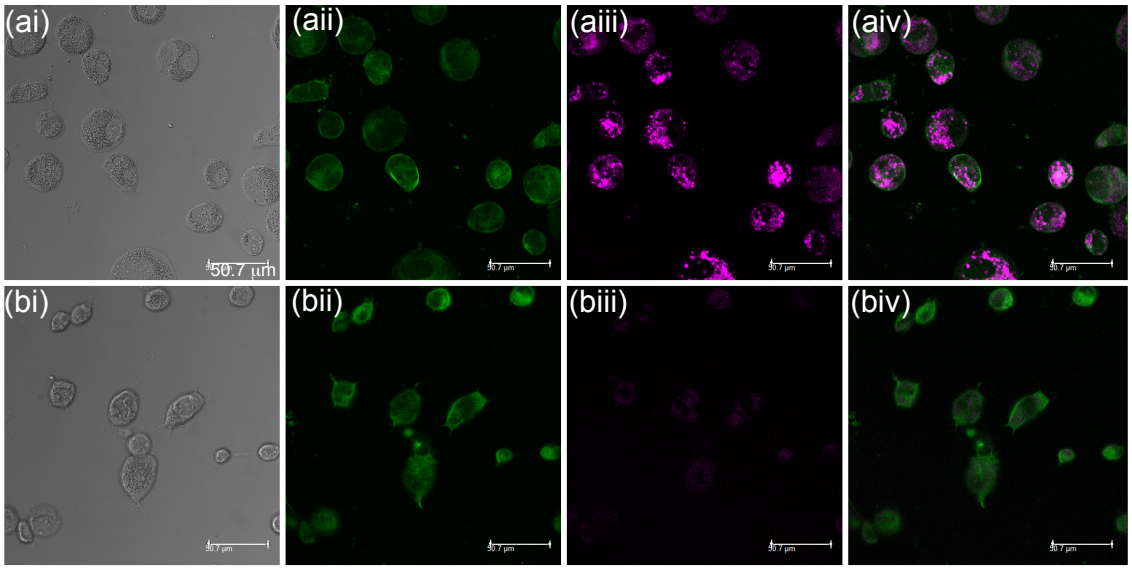

Figure 6. Confocal images of SKOV-3 cells after incubation with **4** (a), **5** (b), at 0.5 µM for 23 h. Tubulin tracker green (1 µM) was added to all wells 45-60 min before taking images; (i) bright-field image, (ii) excitation at 488 nm and emission filter at 500 - 550 nm, (iii) excitation at 633 nm and emission filter at 650 - 800 nm, (iv) overlap of ii and iii.

Nearly homogenous staining was observed throughout the cytosol in both images (aii and bii). This is a typical staining pattern of tubulin tracker green.[62] However, **4** showed uneven and vesicular localization pattern around the nuclei (Fig. 6aiii), similar to lysosomal or endosomal staining patterns.[63, 64] Emission of **5** from the cells was weak, but showed a pattern similar to that of **4**. Tubulin tracker green and the two prodrugs showed very different subcellular localization patterns as observed in the enlarged image (Fig. S16) Thus, we concluded that these two prodrugs did not specifically bind to microtubules inside cells, consistent with the results from the tubulin polymerization assay.

The lower emission of **5** might be due to the lower uptake or quenching of the fluorescence by aggregation. Both prodrugs had limited solubility in aqueous solution ($logD_{7.4} > 3.1$). Thus, we dissolved the prodrugs in DMSO for cellular studies. During the photo and dark toxicity experiments, we had no problems using the DMSO stock solutions. However, the initial subcellular localization study using the DMSO stock solutions was unsuccessful for both prodrugs, presumably due to aggregation. To improve the solubility in the media, we used Tween 80 (1%) in dextrose (5%) solution for the dilutions, which improved the fluorescence signal of both prodrugs in the confocal imaging. However, the emission of **5** was much lower than that of **4**. Although the $logD_{7.4}$ of these prodrugs were not distinguishable, compound **5** seemed to have a lower solubility in aqueous medium than **4**. Compound **5** showed much lower emission than **5** at equimolar concentrations in both Tween 80 (1%)/dextrose (5%) solution and DMEM (Fig. S17).

Stability of 4 and 5 with the SKOV-3 Cells. To see the impact of the cells on PTX release during the *in vitro* study, stability of the two prodrugs in the SKOV-3 culture media was determined in the dark. The two prodrugs were quantified by HPLC after 24 and 72 h incubation in the cell culture medium. The retention times of **4** and **5** were 32 and 21 min in the HPLC chromatograms, respectively (Fig. 3). The calibration curves suggested a linear relationship between the peak area and concentration in the range of 0.1 to 5 μM (70 μL injection, Fig. 7a). The equation of the regression line is $y = 0.513x + 89.22$ (r^2=0.995) and $y = 0.316x + 73.28$ (r^2=0.994) for **4** and **5**, respectively. Total recovered percentiles of **4** and **5** from the culture medium and cells are shown in Figure

7b. Small reductions of 4.9% for **4** and 3.1% for **5**, were found after 3 day incubation. The data suggest that both prodrugs are stable in the dark for at least 3 days, even with the cells.

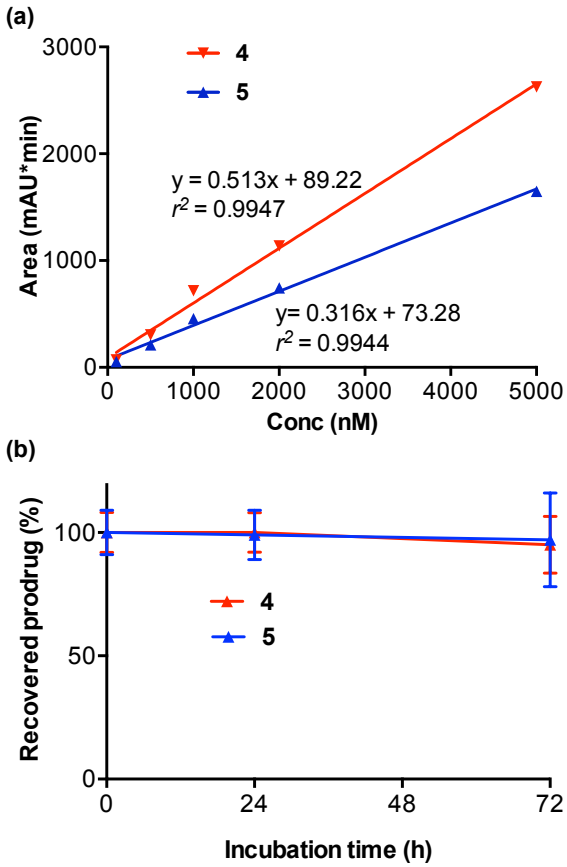

Figure 7. (a) Calibration curves of **4** and **5** based on HPLC. (b) Recovered **4** and **5** from the cell culture medium (cells + culture medium) 24 and 72 h after the addition of prodrugs (500 nM).

Dark and Phototoxicity. Based on the above results - the masking of the tubulin polymerization effect of PTX, efficient photo-release of PTX from **4**, and good stability in the culture medium - we expected low dark toxicity for both prodrugs and high phototoxicity of **4** due to the released PTX by the illumination. Cells were treated with

PTX, **4**, or **5**. Then, cell survival was determined using MTT, with or without illumination using a 690-nm diode laser at 5.6 mW/cm^2 for 30 min.

PTX itself showed potent cytotoxicity against SKOV-3 cells with IC_{50} of 4.7 nM (red lines in Fig. 8), which is close to the reported data.[65] However, both prodrugs **4** and **5** showed dramatically reduced dark toxicity (black lines) with IC_{50} of 910 nM and 1279 nM, 190- and 270- fold reductions from the IC_{50} of PTX, respectively. Once illuminated, both prodrugs showed strong cytotoxicity (green lines) with IC_{50} of **4** and **5** being 3.9 and 24 nM. Since **5** cannot release PTX upon illumination and it is stable in the culture medium, its phototoxicity should have come from its PDT effect through singlet oxygen. **5** seems to be a powerful photosensitizer. The most potent phototoxicity of **4** might come from the combined effects of PDT and released PTX chemotherapy.

To evaluate the contribution of the photo-released PTX in the media to the phototoxicity of **4** and **5**, the culture medium was replaced with fresh medium, called washing. Washing can remove products of the illumination from the media except those in side cells, e.g., released PTX in the media. In both prodrugs, the washing of the parent medium significantly reduced the phototoxicity (blue lines in Fig. 8): IC_{50} of 89 and 53 nM for **4** and **5**, respectively. While there was an ~2-fold reduction in IC_{50} for **5**, an ~23-fold reduction was observed for **4**. The dramatic decrease in the phototoxicity of **4** should have come from the removal of the released PTX from the medium. This finding supports the combined contributions of PDT and released PTX to the phototoxicity of **4**.

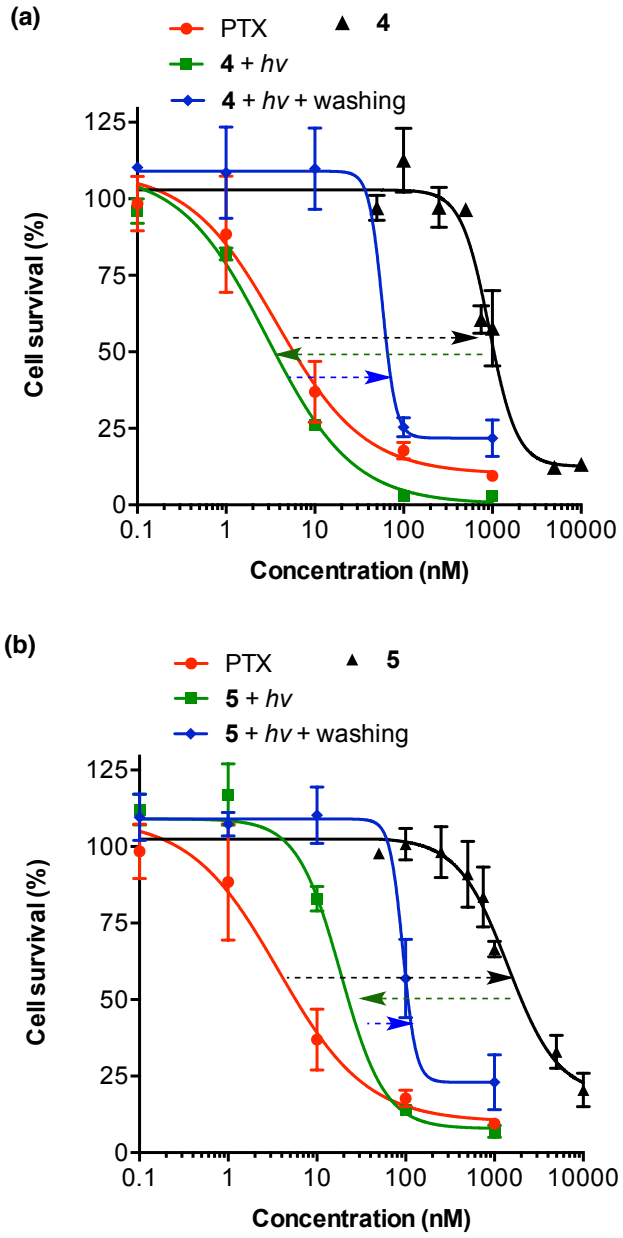

Figure 8. Dark and phototoxicity of **4** (a) and **5** (b) against SKOV-3 ovarian cancer cells, PTX cytotoxicity, and prodrug phototoxicity.

CONCLUSIONS

We designed a light-activatable prodrug of PTX that can express both PDT and chemotherapeutic effects at the illuminated area. The PTX prodrug **4** and its pseudo-

prodrug **5** were readily prepared using a facile synthetic scheme with mild reaction conditions and moderate yields. The activity of PTX was effectively shielded in the prodrugs. However, once illuminated, **4** released a high yield of intact PTX, which caused damage to cancer cells in addition to the immediate effects of PDT. Thus, *in vivo* studies for preclinical optical imaging, toxicity, and antitumor efficacy determinations are warranted. We are currently screening various formulations for an animal study to improve the solubility of these highly lipophilic prodrugs.

This study presents two key significant findings regarding light-activated prodrugs. First, this is the first investigation demonstrating that PTX prodrug can be activated using far-red light and can express both PDT and chemotherapeutic effects simultaneously. PTX is one of the most successful chemotherapeutic drugs in the clinic, and far-red can be easily adopted in the clinic due to its non-toxicity and tissue penetrability. We believe this approach has excellent potential for clinical translation to treat localized tumors. Second, this work demonstrates the applicability of our photo-unclick chemistry (singlet oxygen-mediated release of aminoacrylate type-linkers to drugs) with an aliphatic secondary alcohol. Thus far, we have primarily demonstrated photo-unclick chemistry with phenolic compounds. These results show the applicability of our strategy to broader drugs and bioactive compounds with an aliphatic alcohol, which is a common functional group.

EXPERIMENTAL SECTION

Chemicals and equipment. The starting materials and reagents obtained from Aldrich Chemical co., Fisher Scientific, and VWR were analytical or ACS grades and

were used without further purification. HPLC grade solvents were purchased from Pharmco-AAPER. The products in the syntheses were visualized on thin layer chromatography (TLC plates, cat # Z193291, Sigma-Aldrich) under UV light. Column chromatography was carried out in 40-63 mm (230-400 mesh) silica gel purchased from SiliCycle Inc. (cat # R10030B). NMR spectra were recorded on a Varian 300 MHz spectrometer. The data were analyzed using iNMR (Version 5.4.2) and the chemical shifts were calibrated according to the residual solvent peaks. Chemical shifts were (δ) recorded in ppm with coupling constants (J) in hertz (Hz). Agilent 1260 series HPLC system (Agilent Technologies, USA) was used to quantify PTX, Pc-(L-PTX)$_2$, and Pc-(NCL-PTX)$_2$. A BDS Hypersil C18 column (250 × 4.6 mm, 5-μm particle size) was used with a Pinnacle DB C18 guard column (10 × 4 mm, 5-μm particle size). HRMS was analyzed using an ABSciex QSTAR Elite hybrid quadrupole/TOF mass spectrometer. UV-Vis Lambda 25 (Perkin Elmer) and a 10-mm optical path length quartz cuvette were used for UV-Vis absorption spectra. The fluorescence was monitored in an LS50B spectrometer (Perkin Elmer).

Synthesis. Compound **2** (Scheme 1) was prepared according to the previously reported method.[42] HPLC revealed >95% purity of **4** and **5**, which were used for biological tests.

Compound 1. This compound was prepared based on the previous report with a minor modification.[55] We added propiolic acid (36.9 mg, 0.52 mmol, 1.5 equiv) to a stirred solution of PTX (300 mg, 0.35 mmol, 1.0 equiv) in THF (5 mL) at 0 °C under N_2 gas. After stirring for few minutes, we slowly added DCC (73.2 mg, 0.35 mmol, 1.0 equiv) and DMAP (1.2 mg, 0.01 mmol, 0.03 equiv) dissolved in THF (2 mL) at 0 °C

under N_2 gas. The reaction mixture was stirred at 0 °C for 30 min. Stirring continued for 4 h at room temperature. The precipitate was removed by filtration and washed with ethyl acetate. The filtrate was concentrated to obtain a yellow viscous compound that was purified by column chromatography using ethyl acetate and hexane (1:1 v/v) to produce 273 mg (0.30 mmol, 86%) of compound **1** as a white solid. R_f = 0.37 (ethyl acetate/ *n*-hexane = 2:1 v/v). ^{1}H NMR ($CDCl_3$, 300 MH_Z) δ 8.13 (dd, J = 8.7, 1.5 Hz, 2H), 7.73 (dd, J = 8.4, 1.5 Hz, 2H), 7.63-7.58 (m, 1H), 7.54-7.37 (m, 10H), 6.87 (d, J = 9.3 Hz), 6.28 (br s, 1H), 6.27 (t, J = 8.7 Hz, 1H), 6.01 (dd, J = 9.3, 2.7 Hz), 5.68 (d, J = 6.9 Hz), 5.57 (d, J = 2.7 Hz, 1H), 4.97 (dd, J = 9.6, 1.8 Hz, 1H), 4.47-4.41 (m, 1H), 4.31 (d, J = 8.7 Hz, 1H), 4.20 (d, J = 8.4 Hz, 1H), 3.81 (d, J = 6.9 Hz, 1H), 3.04 (s, 1H), 2.61-2.51 (m, 2H), 2.44 (s, 3H), 2.44-2.35 (m, 1H), 2.23 (s, 3H), 2.23-2.16 (m, 1H), 1.91 (s, 3H), 1.90-1.84 (m, 1H), 1.68 (s, 3H), 1.29 (br s, 1H), 1.25 (s, 3H), 1.13 (s, 3H); ^{13}C NMR δ 203.8, 171.3, 169.8, 167.1, 167.0, 151.4, 142.6, 136.5, 133.7, 133.5, 132.9, 132.1, 130.2, 129.2, 129.1, 128.7, 128.7, 127.1, 126.52, 84.4, 81.1, 79.2, 77.5, 76.6, 75.5, 75.3, 75.1, 73.4, 72.3, 72.1, 58.5, 52.5, 45.52, 43.2, 35.5, 35.5, 26.8, 22.7, 22.2, 20.8, 14.8, 9.6.

Compound 3. This compound was prepared based on the previous report with a minor modification.[56, 57] At room temperature, we slowly added 3.5 mL pyridine to a stirred solution of compound PTX (1.5 g, 1.75 mmol, 1.0 equiv) and succinic anhydride (0.263 g, 2.64 mmol, 1.5 equiv) in dichloromethane (70 mL). The reaction mixture was stirred at room temperature for 24 h under N_2 gas. Then, the mixture was concentrated to give a white solid. The residue was purified by silica gel column chromatography using ethyl acetate and hexane as eluents (1:1 to 8:1 v/v) to produce 1.55 g (1.63 mmol, 93%) of compound **3** as a white solid. R_f = 0.21 (ethyl acetate/ n-hexane = 8:1 v/v). ^{1}H NMR

($CDCl_3$, 300 MH_Z) δ 8.13 (d, J = 7.2 Hz, 2H), 7.73 (d, J = 7.2, 1.5 Hz, 2H), 7.63-7.58 (m, 1H), 7.53-7.48 (m, 10H), 7.03 (d, J = 9.3 Hz), 6.28 (br s, 1H), 6.27 (t, J = 8.4 Hz, 1H), 5.99 (dd, J = 9.0, 2.7 Hz, 1H), 5.68 (d, J = 6.6 Hz, 1H), 5.53 (d, J = 3.0 Hz, 1H), 4.97 (d, J = 8.7 Hz, 1H), 4.46-4.40 (m, 1H), 4.31 (d, J = 8.4 Hz, 1H), 4.20 (d, J = 8.4 Hz, 1H), 3.80 (d, J = 6.6 Hz, 1H), 2.77-2.50 (m, 6H), 2.43 (s, 3H), 2.44-2.31 (m, 1H), 2.21 (s, 3H), 2.17-2.12 (m, 1H), 1.90 (br s, 4H), 1.83 (br s, 1H), 1.67 (s, 3H), 1.22 (s, 3H), 1.12 (s, 3H); ^{13}C NMR δ 203.8, 171.2, 171.0, 169.9, 167.9, 167.2, 167.0, 142.7, 136.8, 133.7, 133.5, 132.7, 132.0, 130.2, 129.1, 129.1, 128.7, 128.7, 128.5, 127.2, 126.5, 84.4, 81.1, 79.1, 76.4, 75.6, 75.1, 74.2, 72.1, 71.9, 58.5, 52.7, 45.6, 43.1, 35.5, 28.8, 28.4, 26.8, 22.6, 22.1, 20.8, 14.8, 9.6.

Compound 4. We slowly added compound **2** (80 mg, 0.10 mmol, 1.0 equiv) dissolved in THF to a stirred solution of compound **1** (218 mg, 0.24 mmol, 2.4 equiv) in dry THF (5 mL) at 0 °C. The reaction mixture was stirred at 0 °C for 1.5 h. Then, THF was evaporated to give a blue solid. The residue was purified by column chromatography using ethyl acetate and n-hexane (2:1, v/v) followed by dichloromethane and methanol (20:1, v/v) to yield 119 mg (0.045 mmol, 46%) of **4** as a blue solid. R_f = 0.21 (dichloromethane/ methanol = 20:1 v/v). ^{1}H NMR ($CDCl_3$, 300 MH_Z) δ 9.63 (dd, J = 5.7, 3.3 Hz, 8H), 8.34 (dd, J = 5.7, 3.0 Hz, 8H), 8.11 (d, J = 7.2 Hz, 4H), 7.75 (d, J = 7.2 Hz, 4H), 7.63-7.57 (m, 2H), 7.53-7.29 (m, 20H), 7.07 (d, J = 8.4 Hz, 2H), 6.94 (d, J = 12.9 Hz, 2H), 6.29 (br s, 2H), 6.22 (t, J = 9.0 Hz, 2H), 5.84 (dd, J = 8.7, 4.5 Hz, 2H), 5.66 (d, J = 6.9 Hz, 2H), 5.53 (d, J = 3.9 Hz, 2H), 4.97 (d, J = 9.9 Hz, 2H), 4.47-4.41 (m, 2H), 4.31 (d, J = 8.7 Hz, 2H), 4.29 (d, J = 13.2 Hz, 2H), 4.19 (d, J = 8.4 Hz, 2H), 3.80 (d, J = 6.9 Hz, 2H), 2.60-2.49 (m, 4H), 2.39 (s, 6H), 2.30-2.25 (m, 2H), 2.23 (s, 6H), 2.16 (br s,

8H), 2.09-2.01 (m, 2H), 1.93 (s, 6H), 1.87-1.82 (m, 2H), 1.67 (s, 8H), 1.25 (s, 6H), 1.13 (s, 6H), 0.25 (br s, 8H), -0.54 (br s, 4H), -1.93 (t, J = 4.8 Hz, 4H); ^{13}C NMR δ 203.9, 171.3, 169.8, 169.2, 168.7, 167.0, 166.9, 152.7, 149.2, 143.2, 137.7, 135.8, 133.9, 133.7, 132.4, 131.8, 131.2, 130.2, 129.2, 128.8, 128.7, 128.6, 128.2, 127.1, 126.8, 123.7, 84.4, 81.2, 80.9, 79.2, 77.2, 76.4, 75.6, 75.1, 72.7, 72.1, 71.2, 58.5, 56.6, 53.6, 53.2, 45.6, 43.1, 35.5, 26.8, 22.6, 22.1, 20.9, 14.8, 9.6; HRMS-ESI : *m/z* calcd. for $[C_{144}H_{146}N_{14}O_{32}Si]^{2+}$: 1305.4998, $[M+2H]^{2+}$, found 1305.4999. Purity = 95% (HPLC Chromatogram, Fig. S11).

Compound 5. To a stirred solution of compound **2** (100 mg, 0.13 mmol, 1.0 equiv) in dry dichloromethane (20 mL) we slowly added compound **3** (298 mg, 0.31 mmol, 2.5 equiv) at 0 °C. Then we added EDC·HCl (67 mg, 0.35 mmol, 2.8 equiv), HOBt hydrate (53 mg, 0.35 mmol, 2.8 equiv) and Et_3N (31 mg, 0.31 mmol, 2.5 equiv) at 0 °C. The reaction mixture was stirred at 0 °C for 30 min. Stirring continued for 3.5 h at room temperature. Then, dichloromethane was evaporated to give a blue solid. The residue was purified by column chromatography using ethyl acetate and n-hexane (8:1, v/v) followed by dichloromethane and methanol (40:1 to 20:1, v/v) to give 192 mg (0.072 mmol, 57%) of **5** as a blue solid. R_f = 0.43 (dichloromethane/ methanol = 15:1 v/v). ^{1}H NMR ($CDCl_3$, 300 MHz) δ 9.63 (m, 8H), 8.34 (m, 8H), 8.11 (dd, J = 8.1, 1.2 Hz, 4H), 7.73 (dd, J = 8.1, 1.2 Hz, 4H), 7.62-7.59 (m, 2H), 7.54-7.24 (m, 20H), 7.16 (d, J = 8.1 Hz, 2H), 6.27 (br s, 2H), 6.17 (t, J = 9.0 Hz, 2H), 5.84 (dd, J = 7.5, 3.0 Hz), 5.66 (d, J = 6.9 Hz, 2H), 5.39 (dd, J = 3.9, 1.5 Hz, 2H), 4.97 (d, J = 9.3 Hz, 2H), 4.45-4.39 (m, 2H), 4.31 (d, J = 8.4 Hz, 2H), 4.19 (d, J = 8.4 Hz, 2H), 3.78 (d, J = 6.9 Hz, 2H), 2.55-2.53 (m, 12H), 2.36 (s, 6H), 2.27 (br s, 8H), 2.26-2.00 (m, 6H), 2.21 (s, 6H), 1.89 (s, 6H), 1.81 (br s, 2H), 1.67 (s, 6H), 1.26 (s, 6H), 1.12 (s, 6H), 0.34 (br s, 4H), 0.19 (br s, 4H), -0.62 (t, J

= 4.8 Hz, 4H), -1.93 (t, J = 4.8 Hz, 4H); ^{13}C NMR δ 203.8, 172.1, 171.2, 169.8, 168.4, 168.2, 167.2, 167.0, 149.2, 142.8, 137.2, 135.8, 133.7, 133.6, 132.7, 131.8, 131.1, 130.2, 129.2, 128.9, 128.7, 128.5, 128.4, 127.2, 126.7, 123.7, 84.4, 81.0, 79.1, 76.4, 75.6, 75.0, 74.1, 72.1, 71.6, 58.5, 56.8, 53.3, 51.4, 51.2, 45.5, 44.0, 43.1, 40.6, 35.5, 35.4, 28.9, 27.7, 26.8, 22.6, 22.1, 20.8, 14.8, 9.6; HRMS-ESI : *m/z* calcd. for $[C_{146}H_{150}N_{14}O_{34}Si]^{2+}$: 1335.5104, $[M+2H]^{2+}$, found 1335.4337. Purity = 98% (HPLC Chromatogram, Fig. S12).

LogD$_{7.4}$ determination. The partition coefficient in of n-octanol and phosphate buffer (PBS, pH 7.4) for **4** and **5** was measured following the previously reported method, with some modifications.[43] In brief, the stock solution of the prodrugs was prepared in DMSO (10 mM). The stock solution (10 mL) was added to n-octanol and PBS (1 mL each) in a vial. The mixture was vortexed for 30 min. Then, the mixture was kept in the dark for 3 h for phase separation. Once there was clear phase separation, both layers were collected in different vials. Each layer (100 mL) was diluted to 1 mL of ACN (5% DMSO) and fluorescence spectra (excitation at 615 nm, emission at 680 nm) were taken. We did not detect the signal in the PBS layer in either prodrug. We determined the lowest concentration of the prodrugs that was detectable using the fluorimeter. The logD$_{7.4}$ value was then estimated using the ratio of concentration in n-octanol to lowest detectable concentration.

Release of PTX from the prodrugs after illumination. *Extraction of PTX from the complete medium:* PTX solution (0.5 mL, 20 μ M) in the complete medium prepared from the DMSO stock was added to a centrifuge tube. Dichloromethane (5 mL) was added to the tube and vortexed for 1 min, followed by centrifugation at 3000 rpm for 10 min for phase separation. The upper media layer was carefully removed using a pasteur

pipette. The lower organic solvent layer was then concentrated with a nitrogen flush. The residue was reconstituted in 100% ACN (0.5 mL), filtered through a 0.2-μm PTFE membrane filter, and transferred into a vial. HPLC was performed using the isocratic mobile phase of 60% ACN and 40% 10 mM ammonium acetate in dH_2O (milliQ) at the flow rate of 0.5 mL/min with an injection volume of 10 uL. *Quantification of released PTX from PTX prodrugs*: Prodrug solution (0.5 mL, 10 μM) in complete medium, diluted from the DMSO stock solution, was added to a 3-cm-diameter glass beaker and was illuminated from above with a laser (690 nm, 5.6 mW/cm^2) for 10, 20, or 30 min. We used the beaker to increase the surface area of light exposure. Then, the illuminated sample was transferred into a centrifuge tube by washing the beaker with dichloromethane (5 mL). We followed the same extraction procedure for the PTX sample, described above. *HPLC conditions:* Isocratic mobile phase of 60% ACN and 40% ammonium acetate (10 mM) in dH_2O (milliQ) at a flow rate of 0.5 mL/min with an injection volume of 10 μL.

Stability of 4 and 5 in the Complete Medium under Dark Conditions. A solution (4 mL, 10 μM) of **4** or **5** prepared in the complete medium from the DMSO stock solution was incubated at 37 °C in the dark. The sample (0.5 mL) was taken at various time points (0, 2 h, 24 h, 48 h, 96 h, and 168 h) and extracted with dichloromethane following the same extraction procedure described for PTX. The extracted sample was reconstituted in 0.5 mL of 5% DMSO in ACN and injected into HPLC. HPLC conditions: Isocratic mobile phase of 90% ACN and 10% ammonium acetate (10 mM) in dH_2O (milliQ) at a flow rate of 0.5 mL/min with an injection volume of 10 μL.

Stability of 4 and 5 with the Cells. On day 0, SKOV-3 cells (5000 cells/well) were seeded on 96-well plates and then incubated at 37 °C in 5% CO_2. On day 1, the solution (10 μL of **4** or **5** was added to each well (190 μL) to make a final concentration of 500 nM. Both cells and medium were collected at 24 and 72 h after the addition of the drugs, respectively. The medium was first collected into the centrifuge tube. The cells were digested using trypsin (100 μL) and were then transferred to the centrifuge tube. After washing with fresh medium (200 μL), all liquids were combined into a 10-mL centrifuge tube. Dichloromethane (1 mL) was subsequently added to the tube. The mixture was vortexed for 10 min and centrifuged at 3000 rpm for 30 min. The upper layer was removed and the extraction was repeated once. The organic layers were combined into a clean vial and dried with nitrogen. The extracts were then reconstituted in 5% DMSO in ACN (200 μL). After sonication for 30 min, the samples were filtered through a 0.2-μm PTFE membrane filter. The filtrate (70 μL) was injected into the HPLC with the mobile phase consisting of a mixture of 90% ACN and 10% ammonium acetate in 10 mM dH_2O (milliQ) at a flow rate of 0.5 mL/min. With a diode array detector (DAD), all separations were detected at 675 nm. Calibration curves of **4** and **5** were prepared with final concentrations of 0.1, 0.5, 1, 2, 5, and 10 μM in the complete medium.

Tubulin Polymerization Assay. A tubulin polymerization assay kit (cat # BK011P, Cytoskeleton, Inc.) was used to assess the effect of prodrugs on tubulin polymerization. The experiment was carried out based on the product protocol as described in version 3.0 of the tubulin polymerization assay kit manual. The basic principle is that the increase in number of microtubules gives higher fluorescence due to

the incorporation of a fluorescent reporter into microtubules. Briefly, the test compound **4** or **5** in DMSO was diluted with distilled water. In 96-well plates, a reaction mixture of tubulin and GTP in a buffer solution was added to the test compound to give final concentration of 3 μM. The reaction mixture was incubated at 37 °C. Fluorescence was monitored (excitation = 360 nm and emission = 450 nm) every 2 min for 1 h. PTX and CA4 were used as positive and negative controls, respectively. DMSO solution was used as a vehicle=only control.

Confocal Microscopic Imaging. SKOV-3 cells were maintained in minimum essential medium (α-MEM) supplemented with 10% bovine growth serum, 2 mM L-glutamine, 50 units/mL penicillin G, 50 μg/mL streptomycin, and 1.0 μg/mL fungizone. All procedures were performed under minimal light. SKOV-3 cells were seeded at 1.0 - 1.5× 10^5 cells/well in 24-well plates containing 12-mm diameter cover slips. Cells were then incubated for 24 h using a Sanyo MCO-18AIC-UV incubator. The stock solution of prodrug **4** or **5** diluted with medium to a concentration of 500 nM, was added to the plates, and was incubated for 24 h. The cells were stained with tubulin tracker green 45-60 min before imaging. Briefly, the medium was removed and the cover slips were washed with HBSS. Tubulin tracker green in HBSS was added to make final concentrations of 1 μM. The wells were incubated for 45-60 min at 37 °C in 5% CO_2. Before visualization under the microscope, cover slips were washed three times with HBSS. Three random fields per treatment were imaged under the confocal microscope (Leica SP2 confocal microscope). Images were captured with a 63x 1.2 NA water Corr lens.

Fluorescence intensity measurements. **4** or **5** DMSO stock solution was further diluted in either 1% Tween 80 in 5% Dextrose solution or DMEM. The final concentration was achieved in a black, clear bottom 96-well plate. The plates were incubated at 37 °C for 24 h. Fluorescence intensity was measured using a Molecular Devises SpectraMAX Gemini EM spectrophotometer with excitation at 615 nm and emission at 680 nm. Data were analyzed using SoftMaxPro software version 5.4.1.

Dark and Phototoxicity. On day 0, SKOV-3 cells (5000 cells/well) were seeded on 96-well plates and were then incubated for 24 h. Stock solutions of PTX, **4**, and **5** were prepared in DMSO (2 mM) and diluted with the medium. Prodrug solution (10 μL) was added to each well containing cells in culture medium (190 μL) to create the desired final concentrations. For dark toxicity, plates were incubated for 72 h. Then, the medium was replaced with medium containing 0.5 μg/mL MTT dye. For phototoxicity, after 24 h incubation in the dark, the plates were placed without lids on an orbital shaker (Lab-line, Barnstead International) and were illuminated using a diode laser (690 nm) at 5.6 mW/cm^2 for 30 min to achieve a light dose of 10 J/cm^2. Then, the plates were placed back into incubator for 72 h. In the experiments to determine the impact of washing the released PTX, the medium was replaced with fresh medium after the illumination.

After 72 h incubation, MTT assays were performed. Briefly, the medium was replaced with medium containing 0.5 μg/mL MTT dye. Then, the medium was removed and the cells were dissolved in 200 μL DMSO, and the absorbance of each well was measured at 570 nm with background subtraction at 650 nm. The cell viability was then quantified by measuring the absorbance of the treated wells compared with that of the untreated wells (controls), and was expressed as a percentage. The cell survival curves

were simulated using GraphPad Prism (Version 6.02, GraphPad software, Inc. La Jolla, CA 92037 USA). The inhibition response parameters were calculated based on the following equation:

$$Cell\ survival\% = Bottom + \frac{(Top - Bottom)}{1 + 10^{(\log(IC50 - Conc)\cdot HillSlope}}$$

In this equation, Top and Bottom are plateaus in the units of the Y-axis, Hill Slope represents the steepness of the curves, and IC_{50} is the concentration of agonist that gives a response halfway between Bottom and Top.

Statistical analysis. Student's *t*-test was used for statistical analysis. *P* values less than 0.05 were considered significant.

ASSOCIATED CONTENTS

Supporting Information Availability. The Supporting Information is available free of charge on the ACS Publications website at XXX. Spectral data (^{1}H, ^{13}C-NMR, and UV-Vis) of the selected compounds and HPLC chromatogram of **4** and **5**

AUTHOR INFORMATION

Corresponding Author. *Phone: 405-271-6593 x47473. Email: Youngjae-you@ouhsc.edu.

Author Contributions. All authors participated in manuscript preparation and revision. Pritam Thapa, Moses Bio, and Gregory Nkepang designed the prodrug structures and developed the synthetic scheme for these prodrugs. Pritam Thapa performed stability, photo-release, and $logD_{7.4}$ studies. Mengjie Li evaluated the stability in the culture condition and dark and phototoxicity. Pallavi Rajaputra collected

subcellular images. Yajing Sun and Moses Bio collected the tubulin polymerization data. Youngjae You and Sukyung Woo were involved in the design of project and interpretation of data.

Notes. The authors declare no competing financial interest.

ACKNOWLEDGEMENTS

Research reported in this publication was supported by the National Institute of General Medical Sciences of the National Institutes of Health under award number R01GM113940 and in part by the DoD [Breast Cancer Research Program] under Award Number W81XWH-14-1-0392. The views and opinions of and endorsements by the authors do not reflect those of the U.S. Army or the DoD.

ABBREVIATIONS USED

PTX, paclitaxel; PDT, photodynamic therapy; CA4, combretastatin A-4; Pc, silicon phthalocyanine; L, SO-cleavable aminoacrylate linker; NCL, non-cleavable linker.

REFERENCES

(1) Wani, M. C.; Taylor, H. L.; Wall, M. E.; Coggon, P.; McPhail, A. T. Plant antitumor agents. VI. the isolation and structure of taxol, a novel antileukemic and antitumor agent from Taxus brevifolia. *J. Am. Chem. Soc.* **1971**, *93*, 2325-2327.

(2) Miller, R. W. P., R. G. Smith, C. R. Edward, A. Clardy, J. Antileukemic alkaloids from Taxus wallichiana Zucc. *J. Org. Chem* **1981**, *46*, 1469-1474.

(3) Manfredi, J. J.; Horwitz, S. B. Taxol: an antimitotic agent with a new mechanism of action. *Pharmacol. Ther.* **1984**, *25*, 83-125.

(4) Ozols, R. F.; Bundy, B. N.; Greer, B. E.; Fowler, J. M.; Clarke-Pearson, D.; Burger, R. A.; Mannel, R. S.; DeGeest, K.; Hartenbach, E. M.; Baergen, R.; Gynecologic Oncology, G. Phase III trial of carboplatin and paclitaxel compared with cisplatin and paclitaxel in patients with optimally resected stage III ovarian cancer: a gynecologic oncology group study. *J. Clin. Oncol.* **2003**, *21*, 3194-3200.

(5) Kampan, N. C.; Madondo, M. T.; McNally, O. M.; Quinn, M.; Plebanski, M. Paclitaxel and its evolving role in the management of ovarian cancer. *Biomed. Res. Int.* **2015**, *2015*, 413076.

(6) Kumar, A.; Hoskins, P. J.; Tinker, A. V. Dose-dense paclitaxel in advanced ovarian cancer. *Clin. Oncol. (R. Coll. Radiol.)* **2015**, *27*, 40-47.

(7) Crown, J.; O'Leary, M.; Ooi, W. S. Docetaxel and paclitaxel in the treatment of breast cancer: a review of clinical experience. *Oncologist* **2004**, 9 Suppl 2, 24-32.

(8) Gennari, A.; Guarneri, V.; Landucci, E.; Orlandini, C.; Rondini, M.; Salvadori, B.; Ricci, S.; Conte, P. F. Weekly docetaxel/paclitaxel in pretreated metastatic breast cancer. *Clin. Breast Cancer* **2002**, *3*, 346-352.

(9) Socinski, M. A.; Bondarenko, I.; Karaseva, N. A.; Makhson, A. M.; Vynnychenko, I.; Okamoto, I.; Hon, J. K.; Hirsh, V.; Bhar, P.; Zhang, H.; Iglesias, J. L.; Renschler, M. F. Weekly nab-paclitaxel in combination with carboplatin versus solvent-based paclitaxel plus carboplatin as first-line therapy in patients with advanced non-small-cell lung cancer: final results of a phase III trial. *J. Clin. Oncol.* **2012**, *30*, 2055-2062.

(10) Ramalingam, S. S.; Khuri, F. R. The role of the taxanes in the treatment of older patients with advanced stage non-small cell lung cancer. *Oncologist* **2009**, 14, 412-424.

(11) Burness, M. L.; Obeid, E. I.; Olopade, O. I. Triple negative breast cancer in BRCA1 mutation carriers with a complete radiologic response to neoadjuvant paclitaxel: a case report. *Clin. Breast Cancer* **2015**, *15*, e155-e158.

(12) Glasgow, M. A.; Yu, H.; Rutherford, T. J.; Azodi, M.; Silasi, D. A.; Santin, A. D.; Schwartz, P. E. Neoadjuvant chemotherapy (NACT) is an effective way of managing elderly women with advanced stage ovarian cancer (FIGO Stage IIIC and IV). *J. Surg. Oncol.* **2013**, *107*, 195-200.

(13) Okazawa, M.; Masuhara, K.; Miyoshi, A.; Fujiwara, K.; Ohta, Y.; Yoshino, K.; Kamiura, S.; Tomita, Y. A rare case of ovarian carcinosarcoma successfully treated with the neoadjuvant chemotherapy of paclitaxel and ifosfamide. *J. Obstet. Gynaecol.* **2011**, *31*, 274-275.

(14) Horiguchi, J.; Oyama, T.; Koibuchi, Y.; Yokoe, T.; Takata, D.; Ikeda, F.; Nagaoka, H.; Rokutanda, N.; Nagaoka, R.; Ishikawa, Y.; Odawara, H.; Kikuchi, M.; Sato, A.; Iino, Y.; Takeyoshi, I. Neoadjuvant weekly paclitaxel with and without trastuzumab in locally advanced or metastatic breast cancer. *Anticancer Res.* **2009**, *29*, 517-524.

(15) Palumbo, R.; Sottotetti, F.; Trifiro, G.; Piazza, E.; Ferzi, A.; Gambaro, A.; Spinapolice, E. G.; Pozzi, E.; Tagliaferri, B.; Teragni, C.; Bernardo, A. Nanoparticle albumin-bound paclitaxel (nab-paclitaxel) as second-line chemotherapy in HER2-negative, taxane-pretreated metastatic breast cancer patients: prospective evaluation of activity, safety, and quality of life. *Drug. Des. Devel. Ther.* **2015**, *9*, 2189-2199.

(16) de Groot, F. M.; van Berkom, L. W.; Scheeren, H. W. Synthesis and biological evaluation of 2'-carbamate-linked and 2'-carbonate-linked prodrugs of paclitaxel: selective activation by the tumor-associated protease plasmin. *J. Med. Chem.* **2000**, *43*, 3093-3102.

(17) Elsadek, B.; Graeser, R.; Esser, N.; Schafer-Obodozie, C.; Abu Ajaj, K.; Unger, C.; Warnecke, A.; Saleem, T.; El-Melegy, N.; Madkor, H.; Kratz, F. Development of a novel prodrug of paclitaxel that is cleaved by prostate-specific antigen: an in vitro and in vivo evaluation study. *Eur. J. Cancer* **2010**, *46*, 3434-3444.

(18) Skwarczynski, M.; Hayashi, Y.; Kiso, Y. Paclitaxel prodrugs: toward smarter delivery of anticancer agents. *J. Med. Chem.* **2006**, *49*, 7253-7269.

(19) Schmidt, F. U.; I. Duval, R.; Alain, P.; Monneret, C. Cancer chemotherapy: A paclitaxel prodrug for ADEPT (antibody-directed enzyme prodrug drug therapy). *Eur. J. Org. Chem.* **2001,** *2001*, 2129-2134.

(20) Satsangi, A.; Roy, S. S.; Satsangi, R. K.; Vadlamudi, R. K.; Ong, J. L. Design of a paclitaxel prodrug conjugate for active targeting of an enzyme upregulated in breast cancer cells. *Mol. Pharm.* **2014**, *11*, 1906-1918.

(21) Erez, R.; Segal, E.; Miller, K.; Satchi-Fainaro, R.; Shabat, D. Enhanced cytotoxicity of a polymer-drug conjugate with triple payload of paclitaxel. *Bioorg. Med. Chem.* **2009**, *17*, 4327-4335.

(22) Majoros, I. J.; Myc, A.; Thomas, T.; Mehta, C. B.; Baker, J. R., Jr. PAMAM dendrimer-based multifunctional conjugate for cancer therapy: synthesis, characterization, and functionality. *Biomacromolecules* **2006**, *7*, 572-579.

(23) Stenzl, A.; Burger, M.; Fradet, Y.; Mynderse, L. A.; Soloway, M. S.; Witjes, J. A.; Kriegmair, M.; Karl, A.; Shen, Y.; Grossman, H. B. Hexaminolevulinate guided fluorescence cystoscopy reduces recurrence in patients with nonmuscle invasive bladder cancer. *J. Urol.* **2010,** *184*, 1907-1913.

(24) Bader, M. J.; Stepp, H.; Beyer, W.; Pongratz, T.; Sroka, R.; Kriegmair, M.; Zaak, D.; Welschof, M.; Tilki, D.; Stief, C. G.; Waidelich, R. Photodynamic therapy of bladder cancer - a phase I study using hexaminolevulinate (HAL). *Urol. Oncol.* **2013**, *31*, 1178-1183.

(25) Simone, C. B. 2nd; Friedberg, J. S.; Glatstein, E.; Stevenson, J. P.; Sterman, D. H.; Hahn, S. M.; Cengel, K. A. Photodynamic therapy for the treatment of non-small cell lung cancer. *J. Thorac. Dis.* **2012,** *4*, 63-75.

(26) Kato, H.; Okunaka, T.; Shimatani, H. Photodynamic therapy for early stage bronchogenic carcinoma. *J. Clin. Laser Med. Surg.* **1996**, *14*, 235-238.

(27) Lightdale, C. J.; Heier, S. K.; Marcon, N. E.; McCaughan, J. S., Jr.; Gerdes, H.; Overholt, B. F.; Sivak, M. V., Jr.; Stiegmann, G. V.; Nava, H. R. Photodynamic therapy with porfimer sodium versus thermal ablation therapy with Nd:YAG laser for palliation of esophageal cancer: a multicenter randomized trial. *Gastrointest. Endosc.* **1995**, *42*, 507-512.

(28) Dougherty, T. J. An update on photodynamic therapy applications. *J. Clin. Laser Med. Surg.* **2002**, *20*, 3-7.

(29) Moor, A. C. Signaling pathways in cell death and survival after photodynamic therapy. *J. Photochem. Photobiol. B* **2000**, *57*, 1-13.

(30) Wilson, J. J.; Jones, H.; Burock, M.; Smith, D.; Fraker, D. L.; Metz, J.; Glatstein, E.; Hahn, S. M. Patterns of recurrence in patients treated with photodynamic therapy for intraperitoneal carcinomatosis and sarcomatosis. *Int. J. Oncol.* **2004**, *24*, 711-717.

(31) Lindberg-Larsen, R.; Solvsten, H.; Kragballe, K. Evaluation of recurrence after photodynamic therapy with topical methylaminolaevulinate for 157 basal cell carcinomas in 90 patients. *Acta Derm. Venereol.* **2012**, *92*, 144-147.

(32) Dysart, J. S.; Patterson, M. S. Characterization of photofrin photobleaching for singlet oxygen dose estimation during photodynamic therapy of MLL cells in vitro. *Phys. Med. Biol.* **2005**, *50*, 2597-2616.

(33) Agostinis, P.; Berg, K.; Cengel, K. A.; Foster, T. H.; Girotti, A. W.; Gollnick, S. O.; Hahn, S. M.; Hamblin, M. R.; Juzeniene, A.; Kessel, D.; Korbelik, M.; Moan, J.; Mroz, P.; Nowis, D.; Piette, J.; Wilson, B. C.; Golab, J. Photodynamic therapy of cancer: an update. *CA Cancer J Clin.* **2011**, *61*, 250-281.

(34) Jiang, M. Y.; Dolphin, D. Site-specific prodrug release using visible light. *J. Am. Chem. Soc.* **2008**, *130*, 4236-4237.

(35) Lee, J.; Park, J.; Singha, K.; Kim, W. J. Mesoporous silica nanoparticle facilitated drug release through cascade photosensitizer activation and cleavage of singlet oxygen sensitive linker. *Chem. Commun.* **2013**, *49*, 1545-1547.

(36) Ghosh, G.; Minnis, M.; Ghogare, A. A.; Abramova, I.; Cengel, K. A.; Busch, T. M.; Greer, A. Photoactive fluoropolymer surfaces that release sensitizer drug molecules. *J. Phys. Chem. B* **2015**, *119*, 4155-4164.

(37) Nani, R. R.; Gorka, A. P.; Nagaya, T.; Kobayashi, H.; Schnermann, M. J. Near-IR Light-mediated cleavage of antibody-drug conjugates using cyanine photocages. *Angew. Chem. Int. Ed.* **2015**, *54*, 13635-13638.

(38) Lamb, B. M.; Barbas, C. F. Selective arylthiolane deprotection by singlet oxygen: a promising tool for sensors and prodrugs. *Chem. Commun.* **2015**, *51*, 3196-3199.

(39) Olejniczak, J.; Carling, C.-J.; Almutairi, A. Photocontrolled release using one-photon absorption of visible or NIR light. *J. Control. Release* **2015**, *219*, 18-30.

(40) Hossion, A. M.; Bio, M.; Nkepang, G.; Awuah, S. G.; You, Y. Visible light controlled release of anticancer drug through double activation of prodrug. *ACS Med. Chem. Lett.* **2013**, *4*, 124-127.

(41) Bio, M.; Rajaputra, P.; Nkepang, G.; Awuah, S. G.; Hossion, A. M.; You, Y. Site-specific and far-red-light-activatable prodrug of combretastatin A-4 using photo-unclick chemistry. *J. Med. Chem.* **2013**, *56*, 3936-3942.

(42) Bio, M.; Rajaputra, P.; Nkepang, G.; You, Y. Far-red light activatable, multifunctional prodrug for fluorescence optical imaging and combinational treatment. *J. Med. Chem.* **2014**, *57*, 3401-3409.

(43) Nkepang, G.; Bio, M.; Rajaputra, P.; Awuah, S. G.; You, Y. Folate receptor-mediated enhanced and specific delivery of far-red light-activatable prodrugs of combretastatin A-4 to FR-positive tumor. *Bioconjug. Chem.* **2014**, *25*, 2175-2188.

(44) Murthy, R. S.; Bio, M.; You, Y. J. Low energy light-triggered oxidative cleavage of olefins. *Tetrahedron Lett.* **2009**, *50*, 1041-1044.

(45) Bio, M.; Nkepang, G.; You, Y. Click and photo-unclick chemistry of aminoacrylate for visible light-triggered drug release. *Chem. Commun.* **2012**, *48*, 6517-6519.

(46) Skwarczynski, M.; Noguchi, M.; Hirota, S.; Sohma, Y.; Kimura, T.; Hayashi, Y.; Kiso, Y. Development of first photoresponsive prodrug of paclitaxel. *Bioorg. Med. Chem. Lett.* **2006**, *16*, 4492-4496.

(47) Noguchi, M.; Skwarczynski, M.; Prakash, H.; Hirota, S.; Kimura, T.; Hayashi, Y.; Kiso, Y. Development of novel water-soluble photocleavable protective group and its application for design of photoresponsive paclitaxel prodrugs. *Bioorg. Med. Chem.* **2008**, *16*, 5389-5397.

(48) You, J.; Shao, R.; Wei, X.; Gupta, S.; Li, C. Near-infrared light triggers release of Paclitaxel from biodegradable microspheres: photothermal effect and enhanced antitumor activity. *Small* **2010**, *6*, 1022-1031.

(49) Gupta, S.; Stafford, R. J.; Javadi, S.; Ozkan, E.; Ensor, J. E.; Wright, K. C.; Elliot, A. M.; Jian, Y.; Serda, R. E.; Dixon, K. A.; Miller, J. J.; Klump, S.; Wallace, M. J.; Li, C. Effects of near-infrared laser irradiation of biodegradable microspheres containing hollow gold nanospheres and paclitaxel administered intraarterially in a rabbit liver tumor model. *J. Vasc. Interv. Radiol.* **2012**, *23*, 553-561.

(50) Gropeanu, R. A.; Baumann, H.; Ritz, S.; Mailander, V.; Surrey, T.; del Campo, A. Phototriggerable 2',7-caged paclitaxel. *PLoS One* **2012**, *7*, e43657.

(51) Sharma, S.; Lagisetti, C.; Poliks, B.; Coates, R. M.; Kingston, D. G.; Bane, S. Dissecting paclitaxel-microtubule association: quantitative assessment of the 2'-OH group. *Biochemistry* **2013**, *52*, 2328-2336.

(52) Snyder, J. P.; Nettles, J. H.; Cornett, B.; Downing, K. H.; Nogales, E. The binding conformation of Taxol in beta-tubulin: a model based on electron crystallographic density. *Proc. Natl. Acad. Sci. USA* **2001**, *98*, 5312-5316.

(53) Jimenez-Barbaro, J.; Souto, A. A.; Abal, M.; Barasoain, I.; Evangelio, J. A.; Acuna, A. U.; Andreu, J. M.; Amat-Guerri, F. Effect of 2 '-OH acetylation on the bioactivity and conformation of 7-O-[N-(4 '-fluoresceincarbonyl)-L-alanyl]taxol. A NMR-fluorescence microscopy study. *Bioorg. Med. Chem.* **1998**, *6*, 1857-1863.

(54) Kingston, D. G. Taxol: the chemistry and structure-activity relationships of a novel anticancer agent. *Trends Biotechnol.* **1994**, *12*, 222-227.

(55) Chen, W. L.; Zhang, J. Z.; Hu, J. H.; Guo, Q. S.; Yang, D. Preparation of amphiphilic copolymers for covalent loading of paclitaxel for drug delivery system. *J. Polym. Sci. A Polym. Chem.* **2014**, *52*, 366-374.

(56) Khandare, J. J.; Jayant, S.; Singh, A.; Chandna, P.; Wang, Y.; Vorsa, N.; Minko, T. Dendrimer versus linear conjugate: Influence of polymeric architecture on the delivery and anticancer effect of paclitaxel. *Bioconjug. Chem.* **2006**, *17*, 1464-1472.

(57) Tong, R.; Cheng, J. Drug-initiated, controlled ring-opening polymerization for the synthesis of polymer-drug conjugates. *Macromolecules* **2012**, *45*, 2225-2232.

(58) Flynn, J. M.; Downs, D. M. In the absence of RidA, endogenous 2-aminoacrylate inactivates alanine racemases by modifying the pyridoxal 5'-phosphate cofactor. *J. Bacteriol.* **2013**, *195*, 3603-3609.

(59) Pettit, G. R.; Singh, S. B.; Hamel, E.; Lin, C. M.; Alberts, D. S.; Garcia-Kendall, D. Isolation and structure of the strong cell growth and tubulin inhibitor combretastatin A-4. *Experientia* **1989**, *45*, 209-211.

(60) Lin, C. M.; Ho, H. H.; Pettit, G. R.; Hamel, E. Antimitotic natural products combretastatin A-4 and combretastatin A-2: studies on the mechanism of their inhibition of the binding of colchicine to tubulin. *Biochemistry* **1989**, *28*, 6984-6991.

(61) Pettit, G. R.; Rhodes, M. R.; Herald, D. L.; Hamel, E.; Schmidt, J. M.; Pettit, R. K. Antineoplastic agents. 445. Synthesis and evaluation of structural modifications of (Z)- and (E)-combretastatin A-41. *J. Med. Chem.* **2005**, *48*, 4087-4099.

(62) Wu, Y. C.; Hour, M. J.; Leung, W. C.; Wu, C. Y.; Liu, W. Z.; Chang, Y. H.; Lee, H. Z. 2-(Naphthalene-1-yl)-6-pyrrolidinyl-4-quinazolinone inhibits skin cancer M21 cell proliferation through aberrant expression of microtubules and the cell cycle. *J. Pharmacol. Exp. Ther.* **2011**, *338*, 942-951.

(63) Bergeland, T.; Widerberg, J.; Bakke, O.; Nordeng, T. W. Mitotic partitioning of endosomes and lysosomes. *Curr. Biol.* **2001**, *11*, 644-651.

(64) Matteoni, R.; Kreis, T. E. Translocation and clustering of endosomes and lysosomes depends on microtubules. *J. Cell Biol.* **1987**, *105*, 1253-1265.

(65) Risinger, A. L.; Peng, J.; Rohena, C. C.; Aguilar, H. R.; Frantz, D. E.; Mooberry, S. L. The bat flower: a source of microtubule-destabilizing and -stabilizing compounds with synergistic antiproliferative actions. *J. Nat. Prod.* **2013**, *76*, 1923-1929.

TABLE OF CONTENTS GRAPHIC

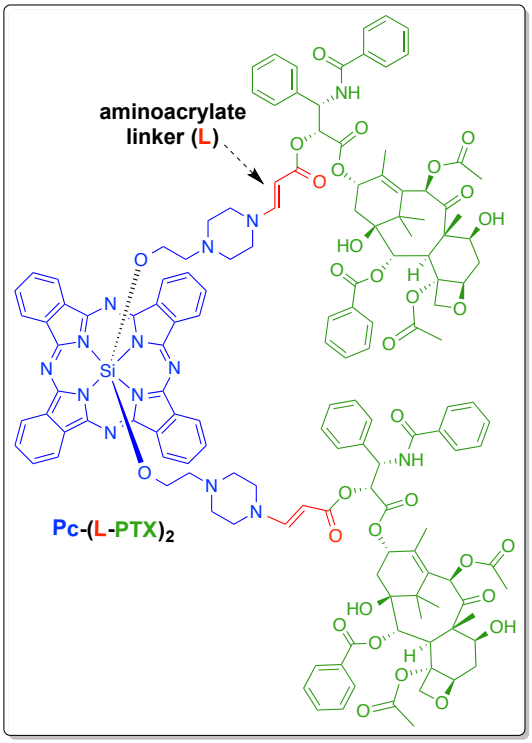

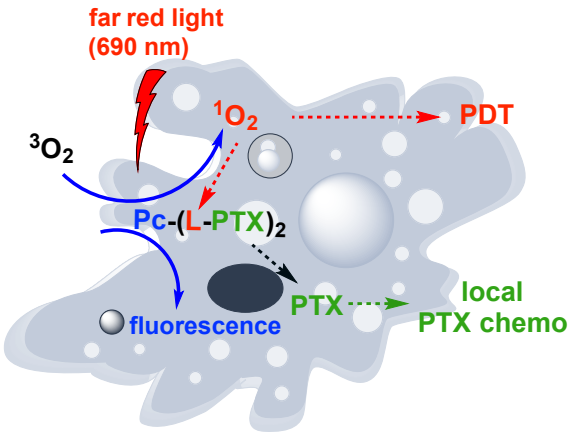

Pc : phthalocyanine
L : $^1O_2$-cleavable aminoacrylate linker
PTX: paclitaxel
PDT: photodynamic therapy